Research article

JHEP|Reports

# Induction of phospholipase A2 group 4C by HCV infection regulates lipid droplet formation

Masahiko Ito[1], Jie Liu[1], Masayoshi Fukasawa[2], Koji Tsutsumi[3], Yumi Kanegae[4], Mitsutoshi Setou[5], Michinori Kohara[6], Tetsuro Suzuki[1,*]

JHEP Reports **2025**. vol. 7 | 1–12



**Background & Aims:** Hepatic steatosis, characterized by lipid accumulation in hepatocytes, is a key diagnostic feature in patients with chronic hepatitis C virus (HCV) infection. This study aimed to clarify the involvement of phospholipid metabolic pathways in the pathogenesis of HCV-induced steatosis.

**Methods:** The expression and distribution of lipid species in the livers of human liver chimeric mice were analyzed using imaging mass spectrometry. Triglyceride accumulation and lipid droplet formation were studied in phospholipase A2 group 4C (*PLA2G4C*) knockout or overexpressing cells.

**Results:** Imaging mass spectrometry of the infected mouse model revealed increased lysophosphatidylcholine levels and decreased phosphatidylcholine levels in HCV-positive regions of the liver. Among the transcripts associated with phosphatidylcholine biosynthesis, upregulation of *PLA2G4C* mRNA was most pronounced following HCV infection. Activation of the transcription factor NF-κB and upregulation of c-Myc were important for activation of *PLA2G4C* transcription by HCV infection and expression of the viral proteins Core-NS2. The amount and size of lipid droplets were reduced in *PLA2G4C*-knockout cells. Inhibition of NF-κB or c-Myc activity suppressed lipid droplet formation in HCV-infected cells. HCV infection promoted the stabilization of lipid droplets, but this stability was reduced in *PLA2G4C*-knockout cells. Overexpression of *PLA2G4C* decreased the levels of phosphatidylcholine species in the lipid droplet fraction and led to lower levels of key factors involved in lipolysis (breakdown of triglycerides into glycerol and free fatty acids), such as ATGL, PLIN1 and ABHD5 on the lipid droplets.

**Conclusions:** HCV infection markedly increases *PLA2G4C* expression. This may alter the phospholipid composition of the lipid droplet membrane, leading to stabilization and enlargement of the droplets.



## Introduction

Hepatitis C virus (HCV) is a major pathogen in chronic liver diseases, including cirrhosis and hepatocellular carcinoma.[1] Hepatic steatosis, characterized by fat deposition within hepatocytes, is also frequently observed in individuals with chronic hepatitis C.[2] HCV protein expression alters cholesterol and lipid metabolism in host cells.[3] HCV core protein disrupts lipid metabolism pathways, contributing to HCV-associated steatosis.[4,5] Additionally, the non-structural proteins NS2, NS4B, and NS5A modulate the expression of genes involved in lipogenesis.[6–8]

Lipid droplets (LDs) are cytoplasmic organelles that store fat and are formed when triglycerides (TG) and cholesterol esters (CE) accumulate between the bilayers of the endoplasmic reticulum membrane. LDs act as hubs for metabolic processes. Notably, HCV utilizes host LDs as scaffolds for viral assembly;[9] increases in LD number and/or size have been observed in cells expressing HCV proteins.[9] The total number of LDs is controlled by the relative balance between lipogenesis and lipolysis. The expression of genes related to lipogenesis and lipolysis, and the activities of their encoded proteins, are involved in the HCV life cycle. Among lipogenesis-related genes, the gene encoding sterol regulatory element binding protein 1c (SREBP-1c) shows increased expression following HCV infection, leading to LD accumulation.[10,11] Diacylglycerol acyltransferases (DGATs) are crucial for endogenous TG biosynthesis and LD formation. DGAT1, a host factor essential for HCV assembly, interacts with the HCV core and NS5A proteins, facilitating their co-loading onto LDs generated via DGAT1's enzymatic activity.[12] Consistent with these observations, knockdown of *DGAT1 and DGAT2* expression decreases neutral lipid content and LD number in virus-infected cells.[13] Other research shows that the expression of lipin1, a key enzyme in glycerophospholipid biosynthesis, is induced by HCV infection, and is involved in forming the membranous web that hosts the HCV replication complex.[14] Among lipolysis-related proteins, α-β hydrolase domain-containing protein 5 (ABHD5) works with adipose triglyceride lipase (ATGL) to mobilize TGs for HCV assembly and infectious particle production.[15,16]

* Corresponding author. Address: Department of Microbiology and Immunology, Hamamatsu University School of Medicine, 1-20-1 Handayama, Higashi-ku, Hamamatsu 4313192, Japan; Tel.: (81)-53-4352336.
*E-mail address:* tesuzuki@hama-med.ac.jp (T. Suzuki).
https://doi.org/10.1016/j.jhepr.2024.101225

Huh-7, a cell line derived from human hepatoma, is permissive for HCV infection. Huh-7 cells were subjected to lipidomic analyses using mass spectrometry (MS) techniques (*e.g.*, liquid chromatography-tandem MS), identifying lipid molecules with altered levels following HCV infection. For example, there was an enrichment of phosphatidylinositol- and phosphatidylcholine (PC)-based lipid species at selected time points of HCV infection.[17,18] Phospholipid monolayers containing PC, phosphatidylethanolamine (PE), and associated proteins surround LDs, and play a key role in the morphogenesis and maintenance of these organelles.[19] Additionally, transcriptome analysis identified mRNA encoding cytosolic phospholipase A2 group 4C (*PLA2G4C*) as a host factor that accumulates following HCV infection. This protein is involved in HCV replication and assembly as well as LD biogenesis.[20,21] PLA2G4C is a member of the phospholipase A2 (PLA2) enzyme family, which hydrolyze glycerophospholipids to produce free fatty acids and lysophospholipids. However, the molecular mechanism by which HCV infection induces changes in LD morphogenesis remains poorly understood.

For the present study, we employed imaging MS (IMS) to characterize the levels of specific lipids in liver tissues. IMS allows visualization of lipid, metabolite, and peptide distributions by defining analysis areas based on images from an optical microscope. The material is then analyzed through laser irradiation of the targeted area. Thus, IMS is suitable for the selective analysis of liver samples from chimeric mice with human liver tissues, which may contain a mixture of human- and mouse-derived tissues.

In the present study, we first used IMS to analyze changes in the levels of PC and lysophosphatidylcholine (LPC) in noncancerous liver tissues from HCV-infected chimeric mice. Specifically, samples were obtained from an HCV infection model created in chimeric (PXB) mice with human liver tissues. We found that LPC levels tended to increase, while PC levels decreased, in regions of the chimeric mouse livers positive for HCV core protein compared to adjacent non-infected sites. Subsequent analysis of cultured human liver cells revealed that, among 32 assayed transcripts encoding factors involved in PC biosynthesis regulation, *PLA2G4C* showed the highest mRNA accumulation following HCV infection. We further demonstrated that the activation of the transcription factors NF-κB and c-Myc by HCV protein expression is crucial for the accumulation of *PLA2G4C* mRNA. This increase in PLA2G4C protein levels led to changes in the phospholipid composition of LDs, resulting in the depletion of lipolysis-related factors associated with the LD surface and increased lipid accumulation within LDs.

## Materials and methods

Detailed materials and methods are provided in the supplementary materials and methods.

## Results

### IMS analysis of HCV-infected human hepatocyte chimeric mice

The mechanism by which HCV infection alters lipid metabolism and composition in liver tissues remains unclear. Therefore, PXB mice were infected with serum from patients with hepatitis C (genotype 1b), and their liver tissues were harvested at 14 and 35 dpi (Fig. 1). Immunohistochemical staining of PXB mouse livers with antibodies against human cytokeratin 8/18 (CK8/18) and mouse cytochrome P450 3A (CYP3A) revealed that approximately 70–80% of the liver was of human origin and interspersed with clusters of mouse-derived cells (Fig. S1). Notably, IMS is particularly useful for the selective analysis of lipid species in human-derived portions of such organs. Immunostaining was performed on serial liver sections of PXB mice to confirm human/mouse tissue identity and HCV protein expression. Using IMS on adjacent serial sections, areas of human origin were quantitatively assessed to determine the distribution of LPC and PC. A typical immunostaining result is shown in Fig. 1A. Notably, LPCs and PCs include diverse molecular species distinguishable by their polar groups and fatty acid compositions. In this study, six LPCs and ten PCs were detected in human-derived tissues from HCV-infected and uninfected mice. Total LPC and PC amounts were calculated for each liver sample. The total LPC levels at 14 and 35 dpi were elevated by 1.04-fold and 1.20-fold, respectively, compared to uninfected mice. Conversely, the total PC levels at 14 and 35 dpi decreased to 0.86-fold and 0.75-fold, respectively, compared to uninfected mice (Fig. 1B). In infected liver tissues, IMS images of HCV core-positive and adjacent non-infected regions showed nominally higher LPC levels and nominally lower PC levels in HCV core-positive areas compared to non-infected areas (Fig. S2). Focusing on individual LPC and PC species in the HCV core-positive areas compared with the non-infected areas, LPC (18:2) levels increased significantly from 14 dpi to 35 dpi (Fig. 1C), while levels of PC (16:1/16:1) and PC (16:0/16:1) decreased significantly over the same period, with differences growing over time (Fig. 1D).

### HCV infection induces accumulation of the PLA2-encoding *PLA2G4C* transcript

Notably, PC species are synthesized via a *de novo* phospholipid synthesis pathway (Fig. S3); the resulting PC species are subsequently hydrolyzed by cytosolic PLA2G4s to generate LPC species. The LPC species are then converted back to PC species by LPC acyltransferase (LPCAT) activity via a recycling pathway. Phospholipid composition is primarily regulated by the balance between PLA2G4s and LPCATs.

To explore the mechanism by which PC levels decrease upon HCV infection, the expression of genes encoding enzymes involved in these pathways was analyzed by quantitative reverse-transcription PCR in HCV J6/JFH-1-infected Huh7.5.1 cells (Fig. 2A and Fig. S3). *PLA2G4C* mRNA, encoding a PLA2G4 family member, accumulated at significantly higher levels in HCV-infected Huh7.5.1 cells than in uninfected cells (Fig. 2A). The change in *PLA2G4C* transcript levels, which exceeded 100-fold at 3 dpi, was the most pronounced among the 32 assessed genes. Similarly, in the livers of HCV-infected PXB mice, the mRNA expression of *PLA2G4C*, but not of another PLA2-encoding gene (*PLA2G4B*), was significantly higher than that in the livers of uninfected chimeric mice (Fig. 2B). No remarkable change was observed in *LPCAT* expression in response to HCV infection in the cell culture model (Fig. 2A).

In the cell lines harboring a knockout of the *PLA2G4C* locus (*PLA2G4C*-KO1 and -KO2) (Fig. S4), the total PLA2 activity in

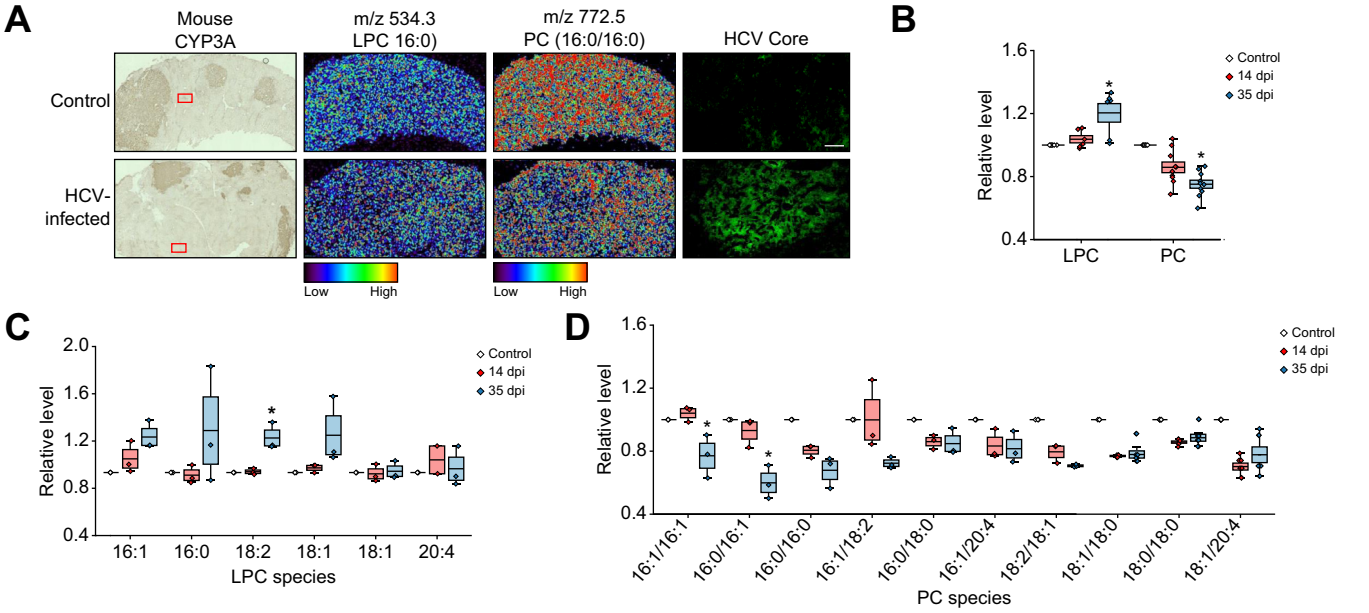


**Fig. 1. IMS of HCV-infected humanized mouse liver samples and quantitative analyses of signal intensities of PC and LPC species.** (A) Liver samples from HCV-infected and non-infected (control) chimeric (PXB) mice were analyzed. Mouse *CYP3A* expression was assessed by immunohistochemical staining (first column). IMS was performed at m/z 534.3 and 772.5 (second and third columns). HCV core expression within the red boxes was detected by immunofluorescence (fourth column). Scale bar: 100 μm. (B) LPC and PC species signal intensities were measured from IMS data in the liver of HCV-infected PXB mice at 14 and 35 dpi, and in uninfected PXB mice (control). Relative levels of mean signal intensities for LPC and PC species are shown. Data are represented as mean ± SEM (n = 4 mice/group, LPC: 6 species, PC: 10 species). The relative levels of LPC and PC species signal intensities are shown in C and D, respectively. Data were analyzed using two-tailed one-way ANOVA with *post hoc* Tukey tests for (B) and T-test with Bonferroni correction (C and D). *$p$ <0.05 *vs.* 14 dpi. Dpi, days post infection; HCV, hepatitis C virus; IMS, imaging mass spectrometry; LPC, lysophosphatidylcholine; PC, phosphatidylcholine.

the cells was significantly lower than that in the parental cells (Fig. 2C). Notably, this deficiency was alleviated in KO cells rescued by the retroviral transduction of *PLA2G4C* (Fig. 2C), whereas transfection of the KO cells with a construct encoding a catalytically inactive PLA2G4C enzyme (G4C/S82A) resulted in a dominant-negative effect, with the transfectant exhibiting decreased PLA2 activity than that of the parent (Fig. 2D). Furthermore, we observed that HCV infection of Huh7.5.1 cells resulted in a significant elevation of intracellular PLA2 activity, which was proportional to the infecting dose (Fig. 2E). We inferred that HCV infection induces the expression of PLA2G4 family members, especially PLA2G4C, leading to an increase in PLA2 activity.

### Mechanism of transcriptional regulation of *PLA2G4C* upon HCV infection

To elucidate the mechanism by which HCV infection potentiates *PLA2G4C* transcript levels, we first expressed each HCV protein alone or various polyproteins in Huh7.5.1 cells and analyzed their effects on *PLA2G4C* mRNA levels (Fig. 3A). The expression of either HCV core-p7 or core-NS2 resulted in an eight-fold or greater increase in *PLA2G4C* mRNA levels. To determine whether *PLA2G4C* transcript accumulation was altered by HCV protein expression in liver tissues (*in vivo*), C57BL/6J mice were administered recombinant adenoviruses encoding HCV core-NS2 or a control GFP protein; then, hepatic *PLA2G4C* transcript levels were assessed. The results showed that HCV core-NS2 expression was associated with a *PLA2G4C* mRNA accumulation of up to 4-fold, whereas the effect on the mRNA level of another PLA2-encoding gene (*PLA2G4B*) was comparable to that observed in mice injected with the control (GFP-encoding) adenovirus (Fig. S5A).

To clarify the regulatory regions and sequences involved in *PLA2G4C* transcript accumulation by HCV infection, promoter reporter vectors were generated, and promoter activity was assessed in Huh7.5.1 cells. The results showed that the expression from the *PLA2G4C* promoter was significantly elevated in response to HCV infection and was proportional to the dose (Fig. 3B). Notably, *PLA2G4C* promoter activity was markedly elevated in cells harboring constructs encoding HCV core-p7 or core-NS2 proteins (Fig. S5B). Partial deletion analyses of the *PLA2G4C* promoter region revealed that the 114 base pairs upstream of the transcription start site are important for activation by HCV infection and viral protein expression (Fig. 3C). *In silico* analysis (not shown) of this promoter region indicated the presence of possible binding sites for the c-Myc, FOXP3, and NF-κB transcription factors. Using *PLA2G4C* promoter reporter constructs, we then demonstrated that introducing point mutations in the predicted binding sites for c-Myc and NF-κB (but not that for FOXP3) in this region attenuated the HCV-induced activation of *PLA2G4C* promoter activity (Fig. 3C). These results suggest that c-Myc and NF-κB are involved in the activation of *PLA2G4C* transcription following HCV infection.

The involvement of NF-κB and c-Myc in transcriptional regulation of the *PLA2G4C* gene was analyzed using the chromatin immunoprecipitation assay, which revealed that HCV infection enhanced NF-κB and c-Myc recruitment to this *PLA2G4C* promoter segment (Fig. 4A). Notably, the recruitment of c-Myc was less pronounced than NF-κB. The potentiation of NF-κB transcriptional activity by HCV infection

**A**

| | MOI | | |
|---|---|---|---|
| | 0.1 | 1 | |
| | Relative to no infection | | *p* value |
| ***De novo* pathway** | | | |
| *GPAM* | 1.02 | 0.9 | 2.66E-01 |
| *GPAT2* | n.d | n.d | |
| *GPAT3* | 1.51 | 2.9 | 7.58E-03* |
| *GPAT4* | 1.31 | 1.9 | 1.02E-02* |
| *AGPAT1* | 1.63 | 2.0 | 4.43E-03* |
| *AGPAT2* | 1.02 | 1.2 | 3.33E-01 |
| *AGPAT3* | 1.36 | 3.4 | 1.96E-04* |
| *AGPAT4* | n.d | n.d | |
| *ABHD5* | 1.20 | 2.1 | 3.50E-03* |
| *GNPAT* | 1.31 | 1.8 | 2.30E-02* |
| *AGPS* | 1.99 | 4.6 | 4.14E-04* |
| *LPIN1* | 1.39 | 1.8 | 9.94E-03* |
| *LPIN2* | 1.48 | 2.4 | 1.69E-03* |
| *LPIN3* | 1.00 | 1.4 | 6.89E-02 |
| *CHKA* | 1.68 | 4.4 | 3.06E-04* |
| *CHKB* | 1.54 | 4.0 | 2.43E-03* |
| *PCYT1A* | 1.16 | 2.0 | 1.14E-03* |
| *PCYT1B* | 1.89 | 1.8 | 1.85E-01 |
| *CEPT1* | 1.40 | 2.7 | 7.29E-03* |
| *CHPT1* | 1.15 | 1.8 | 1.78E-02* |
| **CDP-DAG pathway** | | | |
| *PTDSS1* | 1.14 | 1.4 | 8.79E-02 |
| *PEMT* | 1.33 | 1.9 | 7.65E-03* |
| **Recycling pathway** | | | |
| *LPCAT1* | 1.15 | 1.8 | 2.31E-03* |
| *LPCAT2* | n.d | n.d | |
| *LPCAT3* | 0.80 | 1.0 | 9.63E-01 |
| *LPCAT4* | 1.21 | 1.6 | 2.91E-02* |
| *PLA2G4A* | 1.93 | 5.0 | 1.68E-03* |
| *PLA2G4B* | 1.14 | 2.4 | 2.46E-03* |
| *PLA2G4C* | 18.97 | 104.8 | 5.83E-05* |
| *PLA2G4D* | 0.89 | 2.3 | 1.38E-01 |
| *PLA2G4E* | n.d | n.d | |
| *PLA2G4F* | n.d | n.d | |

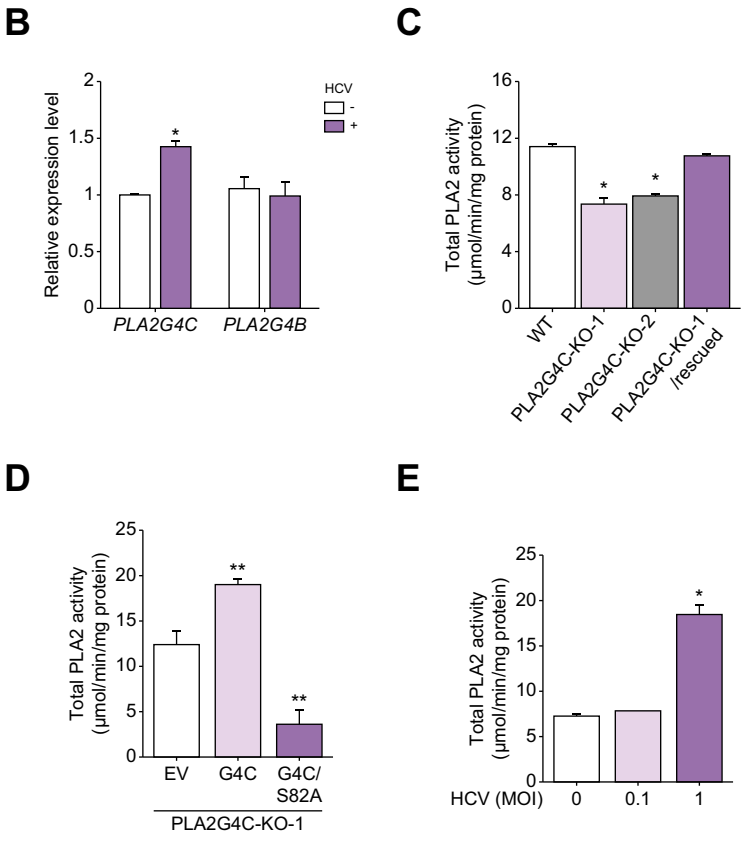


**Fig. 2. Effect of HCV infection on the expression of genes involved in the phosphatidylcholine synthesis and PLA2 activity.** (A) Huh7.5.1 cells were infected with HCV (J6/JFH-1) at MOIs of 0.1 and 1. At 3 dpi, mRNA expression of enzymes involved in phosphatidylcholine synthesis (see Fig. S4) was determined by RT-qPCR, normalized to *GAPDH*, and compared to mock-infected cells (MOI = 0) using a two-tailed unpaired Student's *t* test (*$p$ <0.05). n.d., not determined. (B) RNA from the livers of PXB mice, with or without HCV infection at 14 dpi, was analyzed. (C) Total PLA2 activities were measured in lysates of PLA2G4C-KO cells (PLA2G4C-KO-1, PLA2G4C-KO-2), rescued KO cells (PLA2G4C-KO-1/rescued), and parental Huh7.5.1 cells (WT). (D) PLA2G4C-KO-1 cells were transfected with EV, normal PLA2G4C (G4C)-, or catalytically inactive PLA2G4C (G4C/S82A) expressing constructs. Total PLA2 activities were determined at 3 days post-transfection. (E) Total PLA2 activities were measured in lysates of Huh7.5.1 cells infected with HCV at MOIs of 0.1 and 1, and mock-infected cells, at 2.5 dpi. Data (mean ± SEM, n = 3) were analyzed using two-tailed one-way ANOVA with *post hoc* Tukey tests. *$p$ <0.05, **$p$ <0.01 *vs.* uninfected-, WT-, EV-, and mock infection groups in B-E, respectively. Dpi, days post infection; EV, empty vector; HCV, hepatitis C virus; KO, knockout; MOI, multiplicity of infection; RT-qPCR, quantitative reverse-transcription PCR; WT, wild-type.

was further demonstrated using a NanoLuc reporter plasmid containing an NF-κB response element (Fig. S6A). The NF-κB response element was activated by HCV core-p7 and core-NS2 in Huh7.5.1 cells (Fig. S6B). HCV infection led to decreases in IκB (inhibitor of NF-κB) phosphorylation and protein levels and an increase in phosphorylated p65 levels, indicating activation of the classical NF-κB pathway (Fig. 4B). Consistent with these observations, imiquimod, an NF-κB activator that induces p65 phosphorylation, also resulted in endogenous *PLA2G4C* mRNA accumulation (Fig. 4C). Furthermore, our results showed that imiquimod enhanced *PLA2G4C* promoter activity in a dose-dependent manner, and that this effect was abolished by a point mutation in the predicted NF-κB-binding site in the *PLA2G4C* promoter (Fig. S6C). Exposure to non-cytotoxic concentrations of Bay 11-7082, a known NF-κB inhibitor, also dose-dependently attenuated of HCV infection-induced accumulation of the *PLA2G4C* transcript (Fig. 4D and Fig. S6D).

Notably, c-Myc forms a heterodimer with the Max protein, and the c-Myc/Max complex functions as a transcription factor. In general, Max is abundant in cells and we observed that the levels of this protein did not vary significantly upon HCV infection (data not shown). Therefore, we inferred that the regulation of c-Myc/Max transcriptional activity depends primarily on c-Myc protein level. Consistent with this hypothesis, c-Myc overexpression led to the accumulation of the endogenous *PLA2G4C* mRNA (Fig. 4E) and potentiated *PLA2G4C* promoter activity (Fig. S6E). As demonstrated above (via promoter assays), point mutations in the predicted c-Myc binding site of the *PLA2G4C* promoter significantly attenuated HCV infection-induced activation of the *PLA2G4C* promoter (Fig. S6E). Furthermore, HCV infection of Huh7.5.1 cells resulted in *c-Myc* mRNA accumulation, which was proportional to the HCV titer (Fig. 4F). Furthermore, the expression of HCV core-p7 or core-NS2 in Huh7.5.1 cells resulted in 2.0- and 1.7-fold increases in *c-Myc* mRNA levels, respectively (Fig. S6F). Induction of c-Myc transcriptional activity by HCV infection was confirmed using a reporter plasmid containing a c-Myc-responsive element (Fig. S6G). Together, these results suggested that NF-kB- and c-Myc-mediated transcription

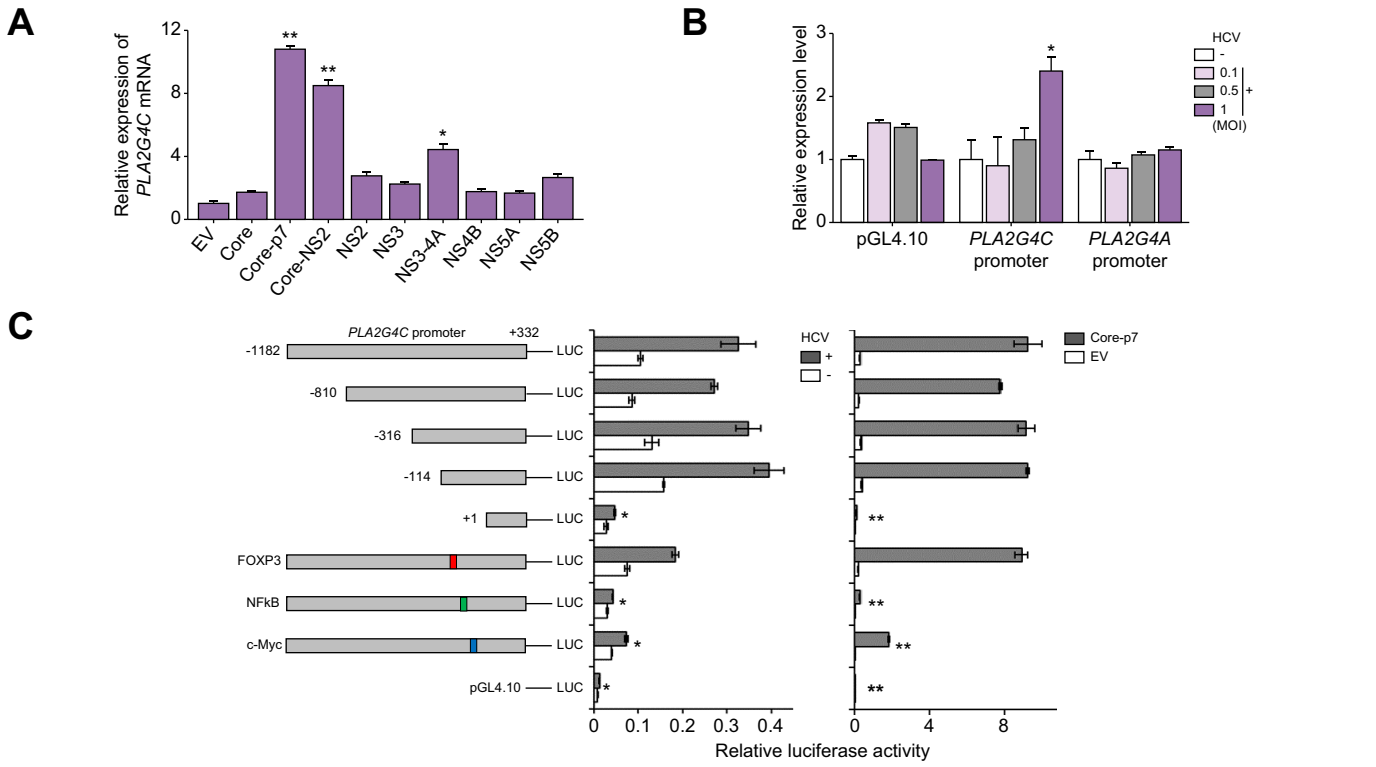


**Fig. 3. Induction of *PLA2G4C* mRNA by HCV proteins, and identification of the *PLA2G4C* promoter region responsible for HCV-mediated transcriptional activation.** (A) Huh7.5.1 cells were transfected with HCV protein-expression plasmids or EV. *PLA2G4C* mRNA levels were determined by RT-qPCR at 2 days post-transfection, normalized to *GAPDH*, and compared to EV-transected cells. (B) Data (mean ± SEM, n=3) were analyzed using two-tailed one-way ANOVA with post hoc Tukey tests. **p* < 0.05, ***p* < 0.01 vs. EV-, mock infection- and PLA2G4C promoter (nt -1182/+332) groups in A-C, respectively. (C) Partial deletions or mutations were introduced within the *PLA2G4C* promoter reporter plasmid. (Left) Huh7.5.1 cells transfected with *PLA2G4C* promoter-firefly luciferase reporter plasmids were infected with HCV (MOI = 0.5). Luciferase activities were measured at 2 dpi. (Right) Huh7.5.1 cells were co-transfected with core-p7 expression plasmid or EV, *PLA2G4C* promoter-firefly luciferase reporter plasmid, and CMV promoter-Renilla luciferase plasmid. Luciferase activities were measured at 3 days post-transfection. Data (mean ± SEM, n = 3) were analyzed using two-tailed one-way ANOVA with *post hoc* Tukey tests. **p* <0.05, ***p* <0.01 *vs*. EV-, mock infection- and PLA2G4C promoter (nt -1182/+332) groups in A-C, respectively. CMV, cytomegalovirus; dpi, days post infection; EV, empty vector; HCV, hepatitis C virus; KO, knockout; MOI, multiplicity of infection; RT-qPCR, quantitative reverse-transcription PCR.

pathways are activated by HCV infection, contributing to the induction of *PLA2G4C* gene expression.

### Involvement of PLA2G4C in HCV production and LD biosynthesis

PLA2G4C is known to be involved in both LD biosynthesis and HCV production.[21] In our analysis of the cell lines harboring mutations in *PLA2G4C*, HCV infection level and the mean fluorescence intensity (MFI) of LD and TG content were decreased in HCV-infected PLA2G4C-KO1 and -KO2 cells compared to parental (non-KO) control cells (Fig. 5A,B and Fig. S7). Retroviral transduction of PLA2G4C in KO cells restored viral RNA levels and MFI of LD and TG content (Fig. 5A,B and Fig. S7), confirming PLA2G4C's role in both the HCV infection cycle and LD biosynthesis. In contrast, an increase in the average fluorescence intensity of LDs with oleic acid addition was observed not only in wild-type (WT) and rescued KO cells, but also in PLA2G4C-KO cells (Fig. 5C and Fig. S8), suggesting that, in these cells, fatty acid uptake is independent of *PLA2G4C* expression. These findings suggested that increased TG levels following HCV infection are likely due to inhibition of the lipolysis pathway rather than upregulation of the lipogenic pathway due to elevated PLA2G4C levels. We further investigated whether LD generation and HCV infection were altered by exposure to small-molecule compounds inhibiting *PLA2G4C* expression. Treatment of HCV-infected WT cells with c-Myc inhibitor 10058-F4 and NF-kB inhibitor BAY 11-7082 reduced HCV RNA levels in cells, whereas no anti-HCV activity was observed in PLA2G4C-KO or rescued KO cells (Fig. 5D and Fig. S9). The reduction of total LD content in WT cells induced by 2.5 μM and 5 μM of 10058-F4 and 2.5 μM of BAY 11-7082 was not observed in PLA2G4C-KO and rescued KO cells (Fig. 5E and Fig. S10). Since the inhibitory effect of these two drugs was not observed in the rescued KO cells in which the *PLA2G4C* gene was not expressed from the native transcriptional regulatory system but from the *EF1α* promoter, 10058-F4 and BAY 11-7082 possibly inhibited *PLA2G4C* promoter activity and reduced its production, resulting in suppression of LD levels and virus production. The reduction of LD content upon 5 μM BAY 11-7082 treatment was observed not only in WT cells but also in the KO and rescued KO cells (Fig. 5E), suggesting that high concentrations of BAY11-7082 effects a factor other than *PLA2G4C*. These data suggested that PLA2G4C inhibitors might be a starting point for developing drugs against HCV-induced steatohepatitis.

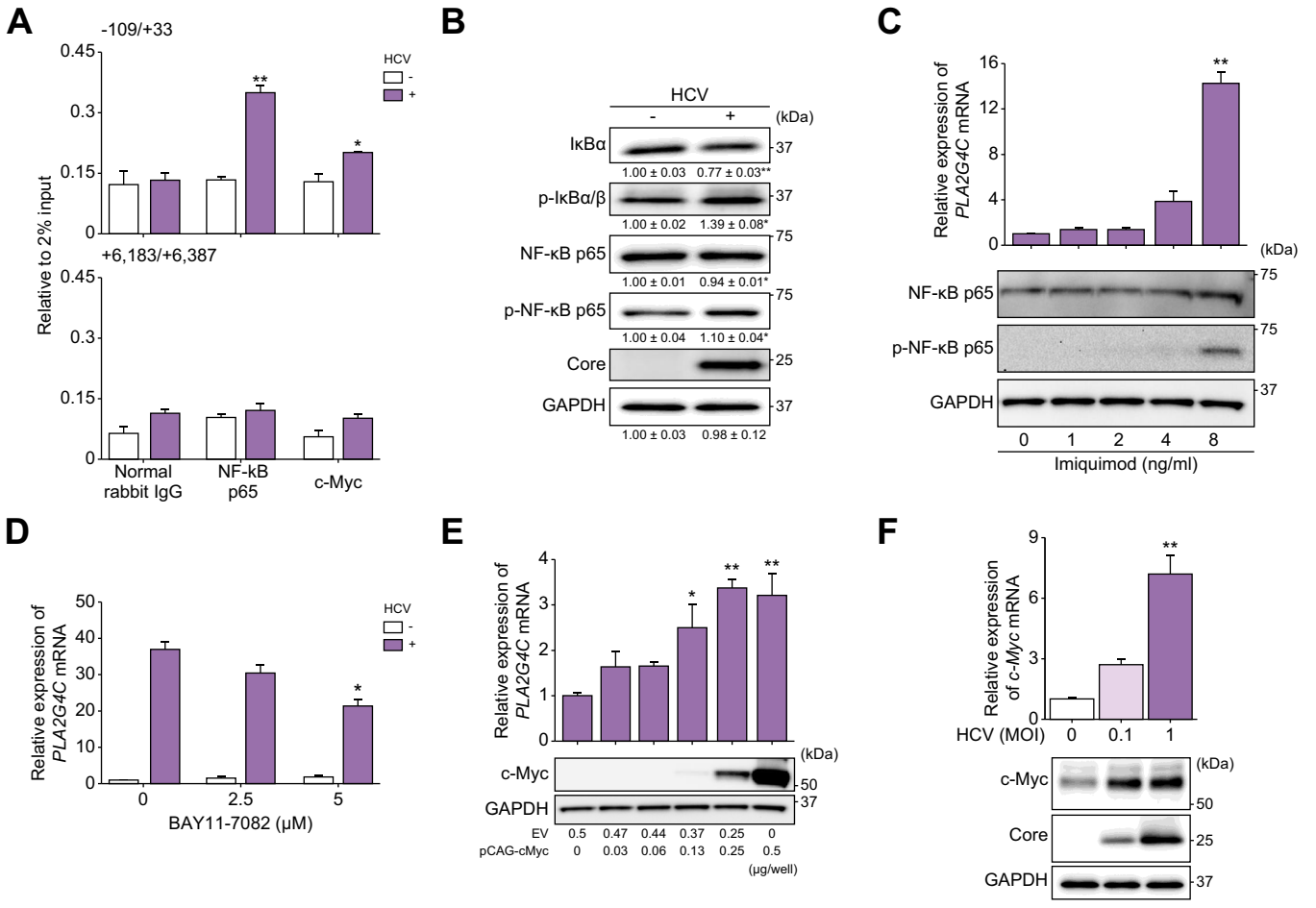


**Fig. 4. Involvement of NF-κB and c-Myc in the transcriptional regulation of *PLA2G4C*.** (A) Huh7.5.1 cells were mock-infected (-) or infected with HCV (+) and harvested at 2.5 dpi. Nuclear fractions were used for chromatin immunoprecipitation with antibodies against NF-κB, c-Myc, or rabbit IgG (control). qPCR targeted the proximal and distal *PLA2G4C* transcription start site. (B) Huh7.5.1 cells were harvested at 2 dpi with or without HCV infection (MOI = 1) for immunoblotting. Protein levels were quantified by ImageJ. The intensity of each band in mock infected cells was set to 1, with relative values for HCV-infected cells. (C) Huh7.5.1 cells were cultured with imiquimod (a NF-κB activator) at different concentrations for 2 days. *PLA2G4C* mRNA levels were assessed by RT-qPCR (upper panel), and NF-κB activation was examined by immunoblotting (lower panel). (D) Huh7.5.1 cells infected or uninfected with HCV were cultured with Bay 11-7082 (a NF-κB inhibitor) at different concentrations for 2 days. *PLA2G4C* mRNA levels were assessed by RT-qPCR. (E) Huh7.5.1 cells were transfected with a c-Myc expression plasmid or EV at different concentrations for 2 days. *PLA2G4C* mRNA levels were assessed by RT-qPCR (upper panel), and c-Myc levels were examined by immunoblotting (lower panel). (F) Huh7.5.1 cells infected with or without HCV at the indicated MOIs were cultured for 2.5 dpi. c-*Myc* mRNA levels were assessed by RT-qPCR. Relative RNA expression values were normalized to those of *GAPDH*. c-Myc induction was examined by immunoblotting (lower panel). Data (mean ± SEM, n = 3) were analyzed using two-tailed one-way ANOVA with post hoc Tukey's tests. **p* <0.05, ***p* <0.01 *vs.* mock infection (A,B and F), no-drug control (C and D) or 0.5 EV (E). Dpi, days post infection; EV, empty vector; HCV, hepatitis C virus; MOI, multiplicity of infection; RT-qPCR, quantitative reverse-transcription PCR.

To elucidate the effects of PLA2G4C and HCV on LD formation, we investigated changes in LD size and number in PLA2G4C-KO or parental Huh7.5.1 cells. Notably, in PLA2G4C-KO cells, the mean LD size was 0.77-fold smaller than that in parent cells, correlating well with a decrease in the MFI of LD (Fig. 6A and Fig. S11), whereas the mean LD number was nominally higher in PLA2G4C-KO cells than in the parental control cells (Fig. 6A and Fig. S11). In contrast, the effect of HCV infection on LD morphology was opposite to that of *PLA2G4C* KO. Specifically, the mean LD size increased following HCV infection compared to uninfected control cells, consistent with the changes in the MFI of LD observed in infected cells, and the mean LD number in infected cells was lower than that in uninfected cells (Fig. 6B and Fig. S12A). This increase in the MFI of LD was observed with overexpression of HCV core-NS2 proteins in WT cells. The LD level further increased when the HCV subgenomic replicon expression plasmid (pHH/SGR-Gluc) was introduced together with the core-NS2 expression plasmid (pCAG/C-NS2) (Fig. 6C and Fig. S12B). This result is consistent with the fact that not only core-NS2 but also NS3/4A expression contributes to the induction of *PLA2G4C* mRNA expression, as shown in Fig. 3A. While *PLA2G4C* KO resulted in a 0.49-fold decrease in the MFI of LD compared to control cells, PLA2G4C-KO cells expressing core-NS2 and harboring the subgenomic construct did not exhibit this attenuation of HCV production until at least 3 days post-transfection (Fig. S13). However, these cells still exhibited nominal attenuation of the increase in the MFI, which were otherwise observed in HCV-infected cells. Together, these results demonstrated that PLA2G4C contributes to the changes in LD production and morphology observed following HCV infection.

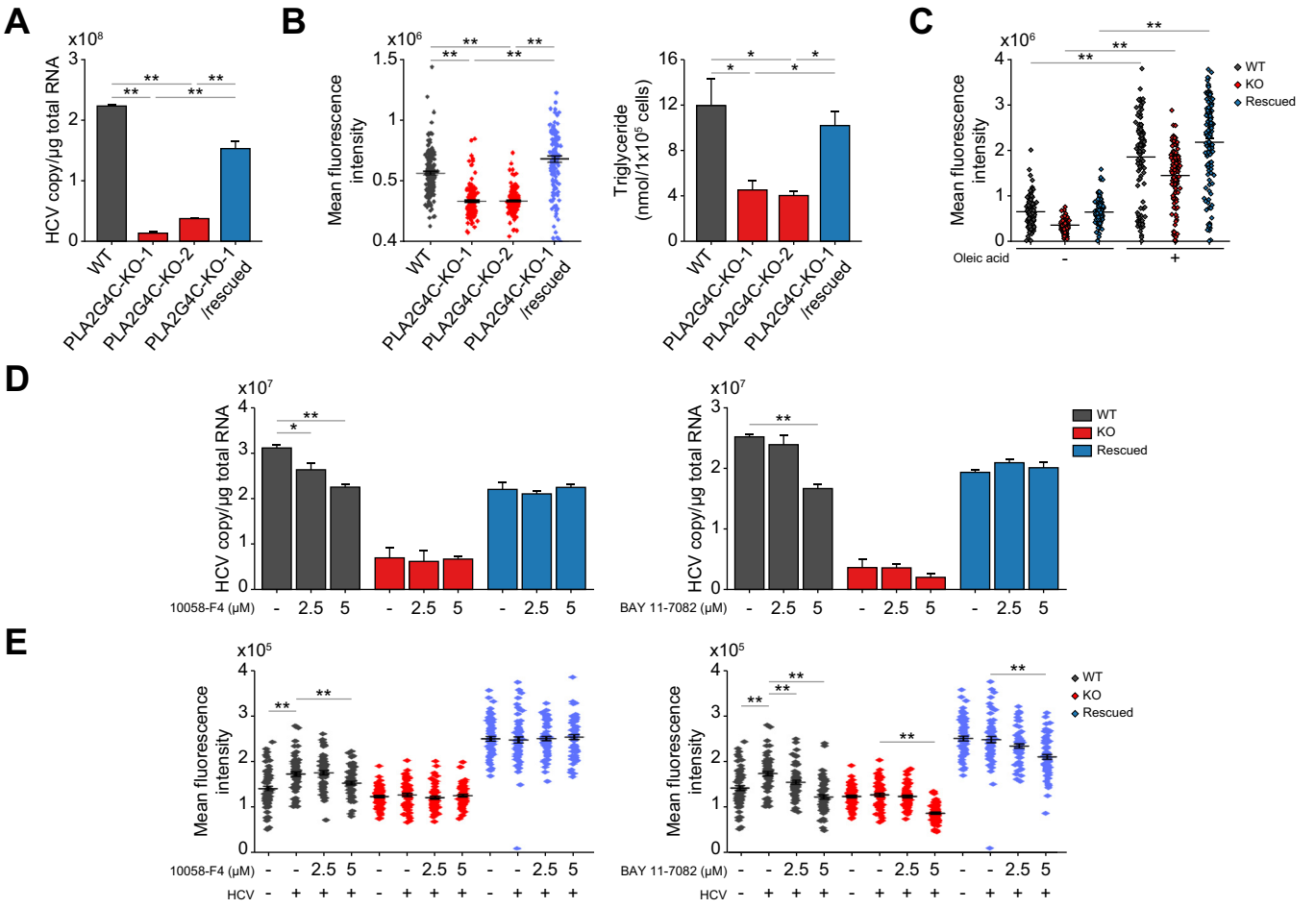


**Fig. 5. Increase in the fluorescence intensity of LD and TG accumulation following PLA2G4C overproduction.** (A) PLA2G4C-KO cells (PLA2G4C-KO-1, PLA2G4C-KO-2), rescued KO cells (PLA2G4C-KO-1/rescued), and parental Huh7.5.1 cells (WT) were infected with HCV (MOI = 1). Intracellular viral RNA was quantified by RT-qPCR at 2.5 dpi. (B) Uninfected PLA2G4C-KO-1, PLA2G4C-KO-2, rescued KO, and WT cells were cultured, fixed, and stained for nuclei and LDs at 1 day. MFIs of LDs were analyzed using an IN Cell analyzer (upper panel). TG levels were determined at 3 days (lower panel). (C) PLA2G4C-KO-1, rescued KO, and WT cells were starved for 12 h, then cultured with (+) or without (-) 94 mg/ml oleic acid-albumin for 12 h. MFI of LDs were analyzed. (D) HCV-infected WT cells, PLA2G4C-KO cells rescued KO were cultured with 10058-F4 (a c-Myc inhibitor) or Bay 11-7082 (a NF-κB inhibitor) for 2 days. Total RNA was assessed for HCV RNA levels. (E) WT cells, PLA2G4C-KO cells, and rescued KO cells were cultured with a c-Myc inhibitor or an NF-κB inhibitor, and the next day, these cells were either infected (+) or uninfected (-) with HCV and harvested at 2 dpi. MFI of LDs were analyzed. Data (mean ± SEM, n = 3) were analyzed using one-way ANOVA with *post hoc* Tukey's tests. **p* <0.05, ***p* <0.01 for comparisons as indicated (A, B and C), or *vs.* the HCV-infected no-drug control (D and E). Dpi, days post infection; HCV, hepatitis C virus; KO, knockout; LD, lipid droplet; MFI, mean fluorescence intensity; MOI, multiplicity of infection; RT-qPCR, quantitative reverse-transcription PCR; WT, wild-type.

### *PLA2G4C* expression induces a decrease in LD localization of lipolysis-related factors

Next, we analyzed the molecular mechanisms by which *PLA2G4C* expression induces changes in LD abundance and morphology. We hypothesized that the enhanced production or suppressed degradation of neutral lipids associated with PLA2G4C activity leads to an increase in the MFI of LD, and that mechanisms such as LD fusion and neutral lipid transfer between LDs are involved in the observed changes in LD size and number. To test this hypothesis, we examined whether *PLA2G4C* expression affected the levels of mRNAs encoding factors involved in the synthesis of neutral lipids, LD budding, and TG transfer. Although *PLA2G4C* overexpression had a limited effect on the mRNA expression of the tested genes, PLA2G4C knockdown increased the mRNA levels of *DGAT1, HMGCR*, *LPIN1*, *LPIN2*, *LPIN3*, *FITM2*, *CIDEB*, *PLIN1* and *PLIN2* by more than 1.5-fold compared to the siControl (Fig. S14), suggesting that *PLA2G4C* expression repressed TG and CE synthesis, TG transfer and/or LD budding. To investigate whether *PLA2G4C* expression or HCV infection is involved in LD stability, we monitored the changes in the MFI of LD over time in Huh7.5.1 cells (both HCV-infected and uninfected) grown with triacsin C, a known inhibitor of TG and CE biosynthesis (Fig. 7A). In HCV-uninfected Huh7.5.1 cells (not mutated for *PLA2G4C*), the MFI of LD slowly decreased after triacsin C addition, decreasing by 15% after 9 h of drug exposure. In contrast, in PLA2G4C-KO cells, nominally greater attenuation of the MFI of LD was observed after triacsin C addition, with values decreasing by 50% after 6 h of drug exposure. No such decrease in the MFI of LD was observed in HCV-infected Huh7.5.1 cells, but a similar decrease was observed in HCV-infected PLA2G4C-KO cells. Overexpression of *PLA2G4C* in Huh7.5.1 cells, which leads to enhanced LD stability, strengthens our hypothesis (Fig. S15A).

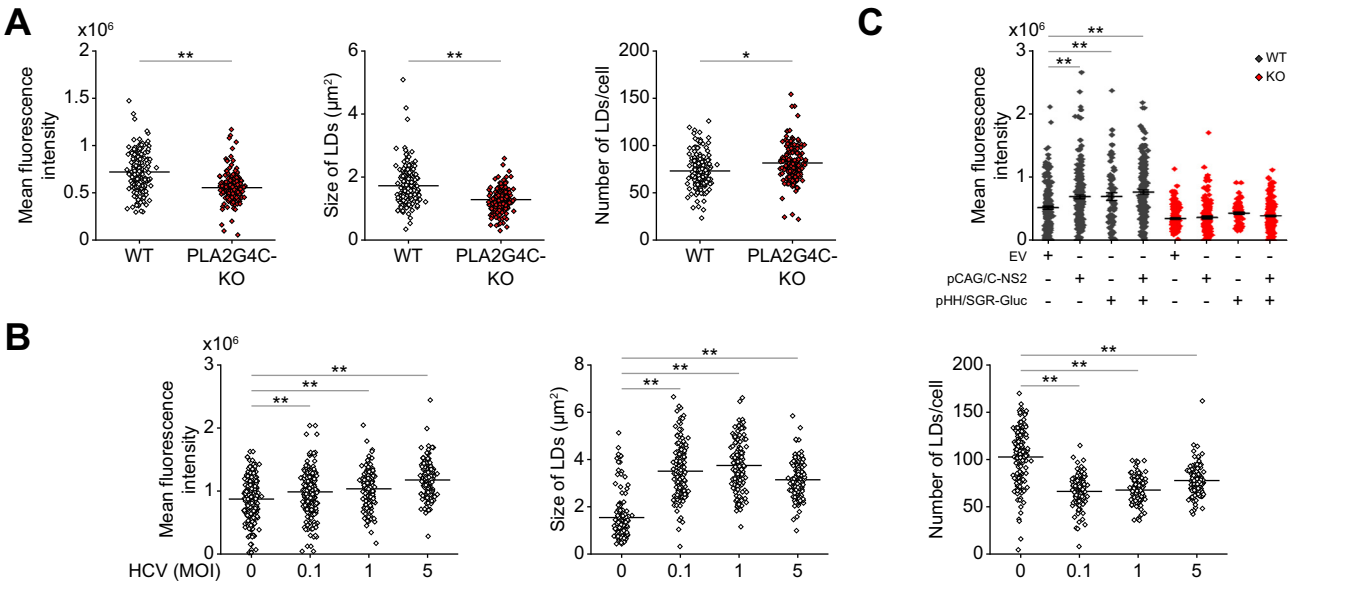


**Fig. 6. LD parameter changes in *PLA2G4C* KO cells or HCV-infected cells.** (A) Uninfected Huh7.5.1 (WT)- and PLA2G4C-KO cells (PLA2G4C-KO-1) were cultured for 1 day, fixed, and stained for nuclei and LDs. LD parameters were analyzed using an IN Cell Analyzer, including 3,693 WT cells and 4,853 PLA2G4C-KO cells. (B) WT cells were infected with HCV at various MOIs. At 2.5 dpi, cells were fixed, stained, and analyzed for LDs. (C) WT and PLA2G4C-KO cells were transfected with EV, pCAG-Core-NS2, pHH/SGR-Gluc, or both. Replicative SGR RNA (genotype 2a) was expressed from pHH/SGR-Gluc under Pol I induction. At 3 dpi, cells were fixed, stained, and analyzed for LDs. Data are presented as mean ± SEM (n = 3). Statistical analysis was performed using two-tailed one-way ANOVA with *post hoc* Bonferroni tests. **p* <0.05, ***p* <0.01 compared as indicated. Dpi, days post infection; EV, empty vector; HCV, hepatitis C virus; KO, knockout; LD, lipid droplet; MOI, multiplicity of infection; SGR, subgenomic replicon; WT, wild-type.

ATGL is a TG lipase responsible for TG degradation and localizes to the LD surface. The activity of this lipase is enhanced by interaction with ABHD5, whose localization is regulated by its interaction with PLIN1. We found that *ATGL*, *ABHD5*, and *PLIN1* transcript levels increased after HCV infection (Fig. S15B), However, these levels did not increase in the cells overexpressing PLA2G4C or its catalytically inactive mutant (Fig. S15C). The effects of c-Myc overexpression or imiquimod treatment on *ATGL*, *PLIN1*, and *ABHD5* transcript levels were further assessed. c-Myc overexpression did not induce these transcripts. While moderate upregulation of *PLIN1* and *ABHD5* mRNA was observed upon imiquimod treatment, the upregulation of their mRNAs was less than 1.5-fold, even in cells treated with 8 ng/ml of imiquimod, which induced a >10-fold increase in *PLA2G4C* expression (Fig. S15D). These results suggested that the mechanism by which mRNA expression of *ATGL*, *PLIN1*, and *ABHD5* is induced by HCV infection differs from that of HCV-mediated PLA2G4C induction. However, PLA2G4C may alter the LD localization of ATGL, ABHD5, and PLIN1. To test this hypothesis, these three factors were expressed as fusion proteins harboring epitope tags, and the cells were subjected to immunofluorescence imaging to analyze the subcellular localization. Confocal microscopy of PLA2G4C-overexpressing cells showed nominal decreases of approximately 40%, 83% and 55% in the LD localization of ATGL, PLIN1, and ABHD5, respectively, than control cells lacking such overproduction (Fig. 7B). Furthermore, decreased levels of endogenous ABHD5 associated with LDs were observed in both HCV-infected and PLA2G4C-overproducing cells compared to control cells (Fig. 7C). However, the expression of endogenous *ATGL* and *PLIN1* were not detected, possibly because of insufficient sensitivity of the antibodies used in Huh7.5.1 cells. In contrast, the level of LD-associated PLA2G4C increased in PLA2G4C-overproducing cells, suggesting that the abundance of PC in these cells may be attenuated in response to increased PLA2 activity in the LD. Consistent with this inference, the LD levels of several PC species were clearly decreased in PLA2G4C-overproducing cells, as assessed by MS of the LD fractions isolated from PLA2G4C-overproducing and control cells (Fig. S16).

Therefore, we speculate that the accumulation of PLA2G4C induced by HCV infection leads to decreased levels of PC species, which are major components of biological membranes, in LDs. This effect leads to a decrease in the association with LDs of membrane proteins, including ATGL, PLIN1, and ABHD5. Additionally, we found that lipase activity decreased after HCV infection or core-NS2 expression (Fig. S17). ABHD5 enhances the lipase activity of ATGL, while PLIN1 regulates the access of ABHD5 to ATGL, thereby controlling its lipase activity on the LD surface. The localization of these proteins at the LD is important for ATGL lipase activity. Collectively, these changes in protein level and/or localization are expected to result in decreased lipolysis efficiency in LDs, leading to stabilization of neutral lipids in these organelles and an increase in LD intensity and size compared to control cells.

## Discussion

Cellular LDs have a neutral lipid core protected from the aqueous environment by a protein-containing phospholipid monolayer. Accelerated LD formation in hepatocytes is a common feature of the liver pathology in patients with chronic HCV infection. Liver tissue from human liver chimeric mice is suitable for studying phospholipid changes because the livers

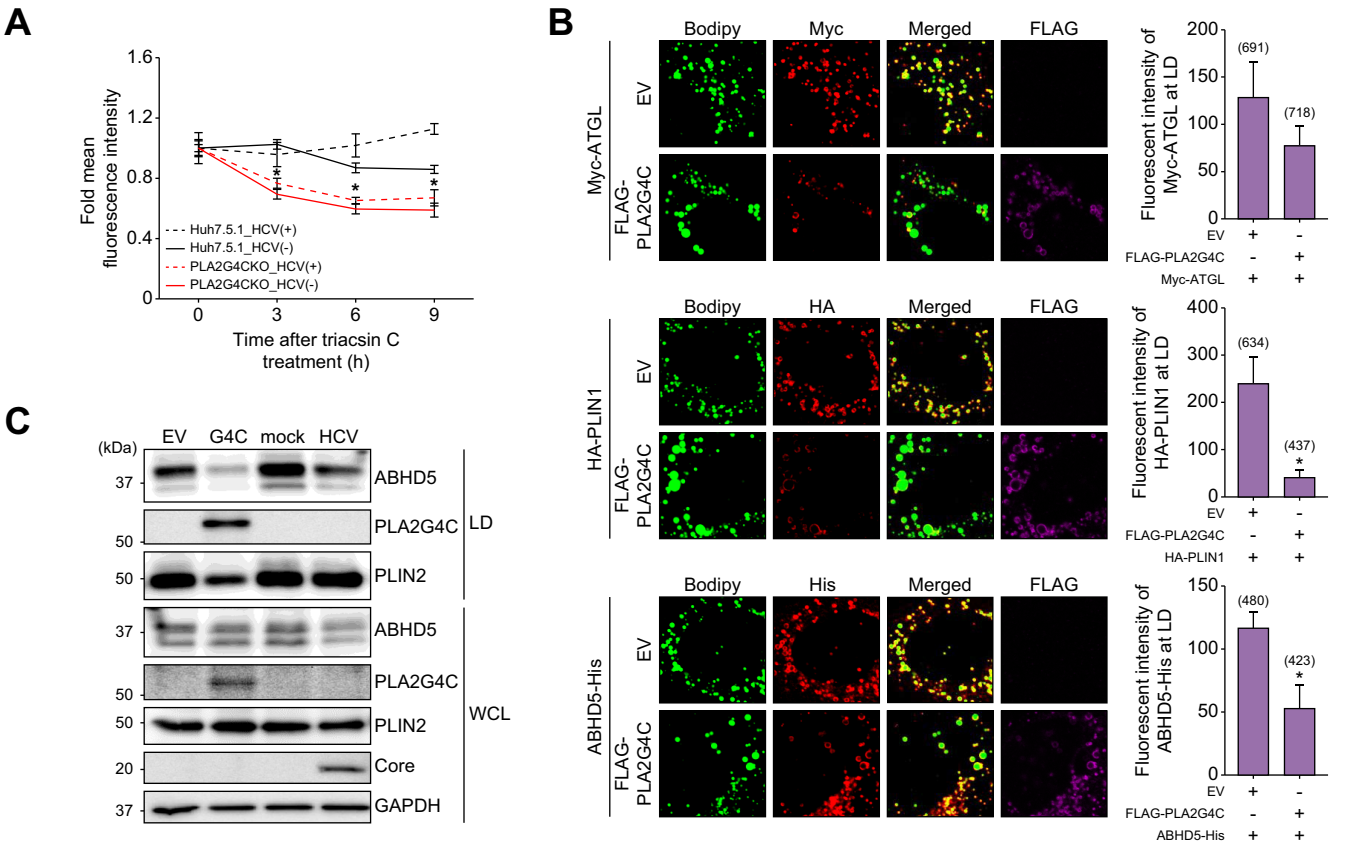


**Fig. 7. Decreases in lipolysis-related proteins associated with LDs following PLA2G4C overproduction.** (A) Huh7.5.1 cells and PLA2G4C-KO cells, with (+) and without (-) HCV infection, were cultured with triacsin C for 9 h. Samples were collected every 3 h, stained for nuclei and LDs, and the MFI of LDs were analyzed using an IN Cell Analyzer. (B) Huh7.5.1 cells were transfected with pCAG-Myc-ATGL, pCAG-HA-PLIN1, or pCAG-ABHD5-His, along with pCAG-FLAG-PLA2G4C or EV. At 2 days post-transfection, cells were fixed, immunostained with antibodies against Myc, HA, His, and FLAG tags, and BODIPY™ 493/503 for LDs, and imaged by confocal laser scanning microscopy; representative images are shown for a sample from each group. Scale bar: 5 μm (Left panel). Fluorescence intensities of Myc-ATGL, HA-PLIN1, and ABHD5-His associated with LDs were analyzed (Right panel). Values in parentheses indicate the numbers of LDs examined. (C) Huh7.5.1 cells were transfected with pCAG-PLA2G4C (G4C) or EV and infected with HCV at MOIs of 0 (mock) or 1 (HCV). At 2 days post-transfection or infection, cells were harvested for immunoblotting of whole cell lysates and LD fractions. Equal amounts of triglycerides (4 μg/lane) were loaded for LD fraction (see Table S4). Data are presented as mean ± SEM (n = 3). Statistical analysis was conducted using two-tailed one-way ANOVA with *post hoc* Tukey's tests. **p* <0.05 *vs*. 0 h (A) or EV (B). EV, empty vector; HCV, hepatitis C virus; KO, knockout; LD, lipid droplet; MFI, mean fluorescence intensity; MOI, multiplicity of infection; RT-qPCR, quantitative reverse-transcription PCR; WT, wild-type.

of such animals exhibit protein expression and lipoprotein cholesterol profiles similar to those of the human liver.[22] Phospholipids, especially PC species, act as physiological solubilizers of cholesterol and are an important component of lipoprotein cholesterol.[23] Based on our findings in chimeric mice and cultured cells, we propose the following model as a mechanism by which HCV infection triggers an increase in LD size in infected cells (Fig. 8). Notably, HCV infection activates NF-κB and c-Myc, and induces *PLA2G4C* transcription. Other studies have shown that oxidative stress contributes to canonical NF-κB activation and increased c-Myc expression, and several HCV proteins increase oxidative stress in the liver and in cultured cells.[24] Increased accumulation of PLA2G4C leads to increased PLA2 activity in HCV-infected cells and the conversion of PC species to LPCs. Notably, PCs are the most abundant phospholipids in LD monolayers, accounting for approximately 60% of total phospholipids in LD membranes. Given that PLA2G4C is localized to cytoplasmic membranes, including LD membranes, increased accumulation of this protein may deplete membrane PCs and alter the dynamic phospholipid-protein interactions that occur on the LD membrane. As a result, the LD membrane localization of TG degradation-related factors (*e.g.*, ATGL, PLIN1, and ABHD5) is decreased, leading to the attenuation of TG degradation in the LD and increased LD size. ATGL and PLIN1 have LD affinity domains,[25,26] and ABHD5 associates with LDs via binding to ATGL or PLIN.[27] The observed change in the PC/LPC ratio presumably leads to changes in the hydrophobicity of the LD surface, resulting in the dissociation of ATGL and PLIN1 from the LD, as well as the release of ABHD5 from these organelles.

LDs are dynamic cellular organelles that dramatically change their volume according to the metabolic state. Although the mechanisms of LD formation and expansion are poorly understood, studies on the link between phospholipid synthesis and LD growth have shown that PC acts as a surfactant and is crucial for stabilizing LDs and preventing their coalescence; attenuation of PC levels leads to larger LDs.[28] Therefore, we infer that HCV infection indirectly promotes LD expansion by inducing PLA2G4C expression, which reduces PC levels and attenuates the inhibitory effect of PC on LD swelling. In

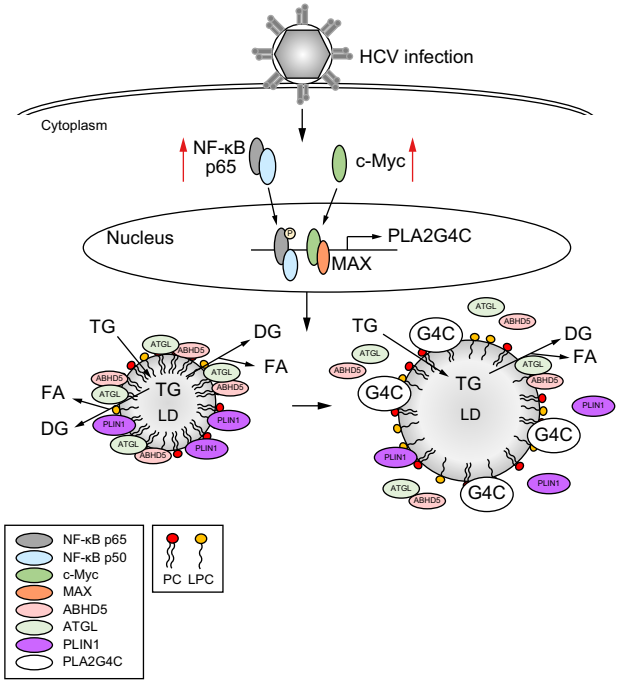


**Fig. 8. Schematic model of PLA2G4C-mediated stabilization and enlargement of LDs in HCV-infected cells.** This model illustrates the mechanism for TG accumulation and LD enlargement in HCV-infected liver tissues. *PLA2G4C* is significantly upregulated (>100-fold) in response to HCV infection, with NF-κB and c-Myc activation as key factors. Increased PLA2G4C leads to enhanced phospholipase activity, depleting membrane PC, altering LD surface hydrophobicity, and reducing the localization of TG degradation-related factors such as ATGL, PLIN1, and ABHD5 to the LD membrane. Consequently, TG degradation in LDs is attenuated, leading to increased LD size. HCV, hepatitis C virus; LD, lipid droplet; PC, phosphatidylcholine; TG, triglyceride.

contrast, PLA2G4A facilitates LD accumulation and core protein envelopment by activating p38 and JNK via arachidonic acid production.[29] However, endogenous PLA2G4A protein is difficult to detect, and GFP-PLA2G4A does not localize to LDs upon HCV infection.[29] Overexpression of *PLA2G4A* in PLA2G4C knockdown cells did not rescue LD formation, indicating distinct roles for PLA2G4C and PLA2G4A in LD dynamics.[21] We found that PLA2G4C is upregulated during HCV infection, localizes to LDs, and suppresses lipolysis, thereby increasing LD content. Despite a 5-fold increase in *PLA2G4A* mRNA expression after HCV infection (Fig. 2A), PLA2G4A may still contribute to LD accumulation to some extent.

The results of the present study are consistent with those of previous reports, indicating that HCV infection increases *PLA2G4C* expression, leading to increased LD production.[20,21] Our work expands on those observations by elucidating the molecular mechanism by which HCV potentiates *PLA2G4C* expression. This study shows for the first time that *PLA2G4C* expression can influence the LD number and size by affecting the PC composition of LD membranes and localization of TG degradation-related factors in the LD membrane. The compositions of PCs and LPCs in the LD fraction were altered by HCV infection and *PLA2G4C* expression, with the strongest effects observed for PC (16:1/20:4) and PC (18:2/18:1) (Fig. S16). Changes in membrane phospholipid content and the PC:LPC ratio are expected to affect membrane morphogenesis, such as membrane curvature. Analysis of the effects of PLA2G4C on the mRNA expression of the genes associated with neutral lipid synthesis, LD budding, and TG transfer showed that the expression of several genes was induced by knockdown but not by overexpression of *PLA2G4C* (Fig. S14), suggesting that the changes in gene expression are not the primary mechanism driving LD formation following HCV infection. Nevertheless, some effects on LD accumulation may exist owing to changes in the expression of lipid metabolism-related genes associated with increased *PLA2G4C* expression following HCV infection.

Metabolic syndrome may have a greater impact on hepatocellular lipid accumulation in chronic viral hepatitis than the virus itself. However, despite most hepatitis C cases with steatosis occurring in individuals of normal weight, patients infected with genotype 3 often exhibit more frequent and higher levels of liver lipid accumulation than those with other genotypes.[30] These observations suggest the direct involvement of HCV in lipid regulatory mechanisms. Several lines of evidence indicate that HCV interacts with LDs in infected cells. For example, the HCV core protein binds to LDs by interacting with DGAT1,[13] and NS5A associates with LDs by binding to PLIN3.[31] While crucial for HCV propagation, the mechanistic role of these HCV-LD interactions in liver disease pathogenesis remains unclear. Our study demonstrated that enhanced PLA2 activity induced by HCV protein expression rather than direct viral protein-LD binding disrupts LD homeostasis. Whether this mechanism varies between HCV genotypes warrants further investigation in future studies.

HCV-related steatosis involves various mechanisms, including activation of lipogenesis pathways, impaired lipoprotein secretion, mitochondrial dysfunction, and membrane lipid peroxidation.[32,33] However, relatively little is known about how HCV infection affects the lipolytic system associated with LD membranes. In addition to the enzymes involved in TG synthesis and storage, lipolytic enzymes (*e.g.* hormone-sensitive lipase, monoacylglycerol lipase, and ATGL) and LD-related proteins (*e.g.* PLIN1, PLIN3, and ABHD5) regulate LD size and number. For instance, PLIN1 inhibits lipolysis by enveloping LDs.[34] Our study revealed that PLA2G4C accumulation causes PLIN1 dissociation from LDs. However, this dissociation from LDs may not have any functional consequences, given that ATGL is also absent from LDs. Although ABHD5 is a major effector of ATGL in adipocytes, its contribution to the lipolytic pathway in hepatocytes remains controversial. Mutations in ABHD5 are the cause of Chanarin-Dorfman syndrome, a neutral lipid storage disorder. Many patients with this condition develop fatty liver disease.[35] Additionally, HCV studies suggest that ATGL and ABHD5 cooperate in LD degradation and HCV morphogenesis.[15] However, changes in phospholipid metabolism have not been shown to affect the regulation or disruption of LD homeostasis via the ABHD5-ATGL axis. Our study demonstrated that the accumulation of *PLA2G4C* mRNA led to a decrease in the LD-associated levels of ABHD5 and ATGL in liver cells, possibly by altering the phospholipid composition of the LD membranes. Since *PLA2G4C* expression is induced by HCV infection, we inferred that LD hypertrophy associated with increased PLA2 activity persists in patients with chronic hepatitis C. The elimination of HCV by direct-acting antiviral treatment in patients with hepatitis C is known to lead to the resolution of lipid metabolism abnormalities, suggesting that host factors whose

expression is induced or activated by infection play a key role in HCV-associated steatosis.

In this study, we demonstrated that NF-κB activation and c-Myc upregulation are involved in the transcriptional induction of *PLA2G4C* following HCV infection. We also found that the addition of NF-κB or c-Myc inhibitors to HCV-infected cells resulted in the attenuation of LD accumulation. NF-κB activation in response to HCV infection involves intricate molecular mechanisms mediated by both viral and host factors. While NF-κB activation by HCV infection has been documented,[36] emerging evidence suggests that the viral proteins, including core, NS4B, NS5A, and NS5B, cause the phosphorylation and subsequent degradation of IκBa, an inhibitory protein that sequesters NF-κB in the cytoplasm.[37–41] To date, NF-κB activation has only been investigated in the context of HCV infection and individual expression of each HCV protein. In this study, we found that the expression of core-p7 polyprotein induced *PLA2G4C* mRNA expression and activated NF-κB and c-Myc, more effectively than that of individual HCV proteins. The accumulation of incompletely cleaved proteins and misfolded molecules during the processing of viral precursor polyproteins that associate with the endoplasmic reticulum membrane is more likely to induce stress leading to NF-κB activation, a downstream event of the unfolded protein response, than the expression of individual proteins in mature forms.[42] In addition, oxidative stress, a major cause of NF-κB and c-Myc activation in liver diseases, is known to be induced not only by HCV infection but also by liver steatosis resulting from lifestyle-related diseases. In patients with non-alcoholic steatohepatitis, oxidative phosphorylation is impaired, resulting in decreased hepatic ATP synthesis and increased reactive oxygen species production. Therefore, investigating whether alcohol- and metabolic fatty liver diseases are accompanied by the molecular events observed during the development of viral hepatitis-related fatty liver – including potentiation of PLA2 activity, changes in the phospholipid composition of LD membranes, and attenuation of LD localization of ATGL and its cofactors – will be interesting.


## Affiliations

[1]*Department of Microbiology and Immunology, Hamamatsu University School of Medicine, Hamamatsu, Japan;* [2]*Department of Biochemistry and Cell Biology, National Institute of Infectious Diseases, Tokyo, Japan;* [3]*Department of Biosciences, Kitasato University, Sagamihara, Japan;* [4]*Core Research Facilities, Research Center for Medical Sciences, The Jikei University School of Medicine, Tokyo, Japan;* [5]*Department of Cellular & Molecular Anatomy, Hamamatsu University School of Medicine, Hamamatsu, Japan;* [6]*Department of Microbiology and Cell Biology, Tokyo Metropolitan Institute of Medical Science, Tokyo, Japan*


## Abbreviations

*ABHD5*, α/β hydrolase domain-containing protein 5; *ATGL*, adipose triglyceride lipase; CE, cholesterol ester; HCV, hepatitis C virus; IMS, imaging mass spectrometry; LD, lipid droplet; LPC, lysophosphatidylcholine; LPCAT, lysophosphatidylcholine acyltransferase; MFI, mean fluorescence intensity; MS, mass spectrometry; PC, phosphatidylcholine; *PLA2G4C*, phospholipase A2 group 4C; *PLIN1*, perilipin 1; TG, triglyceride; WT, wild-type.


## Financial support

This work was supported by grants from the Japan Agency for Medical Research and Development (AMED) under Grant nos. JP23fk0210086h0003, JP23fk0210090s0303, JP22fk0210066h0103, JP22ak0101165h0202 to TS, JP22fk0310507s0601, JP23fk0310507s0602 to MI, and a Grant-in-Aid for Scientific Research (JP18H02661) from the Ministry of Education, Culture, Sports, Science and Technology, Japan to TS. The funders had no role in study design, data collection and analysis, decision to publish, or preparation of the manuscript.


## Conflicts of interest

The authors have no conflicts to report.

Please refer to the accompanying ICMJE disclosure forms for further details.

## Authors' contributions

Masahiko Ito and Tetsuro Suzuki: Study concept and design; Masahiko Ito and Liu Jie: Performing the experiments; Masayoshi Fukasawa, Koji Tsutsumi, Yumi Kanegae, Mitsutoshi Setou, Michinori Kohara: Technical or material support; Masahiko Ito and Tetsuro Suzuki: Drafting of the manuscript; Tetsuro Suzuki: funding acquisition. All authors have access to the study data and have reviewed and approved the final manuscript.

## Data availability statement

The data that support the findings of this study are available from the corresponding author, TS (tesuzuki@hama-med.ac.jp), upon reasonable request.

## Declaration of Generative AI and AI-assisted technologies in the writing process

During the preparation of this work the authors used ChatGPT-4 from OpenAI in order to improve readability and language. After using this tool, the authors reviewed and edited the content as needed and take full responsibility for the content of the publication.


## Acknowledgments

We are grateful to T. Mochizuki for secretarial work and to S. Nomura and M. Yamamoto for their technical assistance in Hamamatsu University School of Medicine. We also thank Dr. Chisari for providing Huh7.5.1 cells. Huh7.5.1 cells and the siblings are the Original Research Materials from Apath, LLC. Microscopy experiments were supported by the Advanced Research Facilities & Services, Preeminent Medical Photonics Education & Research Center, Hamamatsu University School of Medicine.


## Supplementary data

Supplementary data to this article can be found online at https://doi.org/10.1016/j.jhepr.2024.101225.

## References

*Author names in bold designate shared co-first authorships.*


[1] Shepard CW, Finelli L, Alter MJ. Global epidemiology of hepatitis C virus infection. The Lancet 2005;5:558–567. https://doi.org/10.1016/S1473-3099(05)70216-4.

[2] Czaja AJ, Carpenter HA, Santrach PJ, et al. Host- and disease-specific factors affecting steatosis in chronic hepatitis C. J Hepatol 1998;29:198–206. https://doi.org/10.1016/s0168-8278(98)80004-4.

[3] Syed GH, Amako Y, Siddiqui A. Hepatitis C virus hijacks host lipid metabolism. Trends Endocrinology Metabolism: TEM 2010;21:33–40. https://doi.org/10.1016/j.tem.2009.07.005.

[4] Moriya K, Yotsuyanagi H, Shintani Y, et al. Hepatitis C virus core protein induces hepatic steatosis in transgenic mice. J Gen Virol 1997;78:1527–1531. https://doi.org/10.1099/0022-1317-78-7-1527.

[5] Yamaguchi A, Tazuma S, Nishioka T, et al. Hepatitis C virus core protein modulates fatty acid metabolism and thereby causes lipid accumulation in the liver. Dig Dis Sci 2005;50:1361–1371. https://doi.org/10.1007/s10620-005-2788-1.

[6] **Oem JK**, **Jackel-Cram C**, Li YP, et al. Activation of sterol regulatory element-binding protein 1c and fatty acid synthase transcription by hepatitis C virus non-structural protein 2. J Gen Virol 2008;89:1225–1230. https://doi.org/10.1099/vir.0.83491-0.

[7] Zou C, Tan H, Zeng J, et al. Hepatitis C virus nonstructural protein 4B induces lipogenesis via the Hippo pathway. Arch Virol 2023;168:113. https://doi.org/10.1007/s00705-023-05743-4.

[8] Meng Z, Liu Q, Sun F, et al. Hepatitis C virus nonstructural protein 5A perturbs lipid metabolism by modulating AMPK/SREBP-1c signaling. Lipids Health Dis 2019;18:191. https://doi.org/10.1186/s12944-019-1136-y.

[9] Miyanari Y, Atsuzawa K, Usuda N, et al. The lipid droplet is an important organelle for hepatitis C virus production. Nat Cel Biol 2007;9:1089–1097. https://doi.org/10.1038/ncb1631.
[10] Bose SK, Kim H, Meyer K, et al. Forkhead box transcription factor regulation and lipid accumulation by hepatitis C virus. J Virol 2014;88:4195–4203. https://doi.org/10.1128/JVI.03327-13.
[11] **Lerat H**, **Kammoun HL**, Hainault I, et al. Hepatitis C virus proteins induce lipogenesis and defective triglyceride secretion in transgenic mice. J Biol Chem 2009;284:33466–33474. https://doi.org/10.1074/jbc.M109.019810.
[12] Camus G, Herker E, Modi AA, et al. Diacylglycerol acyltransferase-1 localizes hepatitis C virus NS5A protein to lipid droplets and enhances NS5A interaction with the viral capsid core. J Biol Chem 2013;288:9915–9923. https://doi.org/10.1074/jbc.M112.434910.
[13] Herker E, Harris C, Hernandez C, et al. Efficient hepatitis C virus particle formation requires diacylglycerol acyltransferase-1. Nat Med 2010;16:1295–1298. https://doi.org/10.1038/nm.2238.
[14] Mingorance L, Castro V, Avila-Perez G, et al. Host phosphatidic acid phosphatase lipin1 is rate limiting for functional hepatitis C virus replicase complex formation. PLoS Pathog 2018;14:e1007284. https://doi.org/10.1371/journal.ppat.1007284.
[15] Vieyres G, Reichert I, Carpentier A, et al. The ATGL lipase cooperates with ABHD5 to mobilize lipids for hepatitis C virus assembly. PLoS Pathog 2020;16:e1008554. https://doi.org/10.1371/journal.ppat.1008554.
[16] **Camus G**, **Schweiger M**, Herker E, et al. The hepatitis C virus core protein inhibits adipose triglyceride lipase (ATGL)-mediated lipid mobilization and enhances the ATGL interaction with comparative gene identification 58 (CGI-58) and lipid droplets. J Biol Chem 2014;289:35770–35780. https://doi.org/10.1074/jbc.M114.587816.
[17] Islam KU, Anwar S, Patel AA, et al. Global lipidome profiling revealed multifaceted role of lipid species in hepatitis C virus replication, assembly, and host antiviral response. Viruses 2023 Feb;15:464. https://doi.org/10.3390/v15020464.
[18] **Diamond DL**, **Syder AJ**, Jacobs JM, et al. Temporal proteome and lipidome profiles reveal hepatitis C virus-associated reprogramming of hepatocellular metabolism and bioenergetics. PLoS Pathog 2010;6:e1000719. https://doi.org/10.1371/journal.ppat.1000719.
[19] Onal G, Kutlu O, Gozuacik D, et al. Lipid droplets in health and disease. Lipids Health Dis 2017;16:128. https://doi.org/10.1186/s12944-017-0521-7.
[20] Xu S, Pei R, Guo M, et al. Cytosolic phospholipase A2 gamma is involved in hepatitis C virus replication and assembly. J Virol 2012;86:13025–13037. https://doi.org/10.1128/JVI.01785-12.
[21] Su X, Liu S, Zhang X, et al. Requirement of cytosolic phospholipase A2 gamma in lipid droplet formation. Biochim Biophys Acta 2017;1862:692–705. https://doi.org/10.1016/j.bbalip.2017.03.007.
[22] Papazyan R, Liu X, Liu J, et al. FXR activation by obeticholic acid or nonsteroidal agonists induces a human-like lipoprotein cholesterol change in mice with humanized chimeric liver. J lipid Res 2018;59:982–993. https://doi.org/10.1194/jlr.M081935.
[23] Salvioli G, Lugli R. Importance of phospholipids in cholesterol-solubilizing capacity of high-density lipoproteins.. 1987. Berlin, Heidelberg: Springer Berlin Heidelberg; 1987. p. 399–402.
[24] Ivanov AV, Bartosch B, Smirnova OA, et al. HCV and oxidative stress in the liver. Viruses 2013;5:439–469. https://doi.org/10.3390/v5020439.
[25] Rowe ER, Mimmack ML, Barbosa AD, et al. Conserved amphipathic helices mediate lipid droplet targeting of perilipins 1-3. J Biol Chem 2016;291:6664–6678. https://doi.org/10.1074/jbc.M115.691048.
[26] Targett-Adams P, Chambers D, Gledhill S, et al. Live cell analysis and targeting of the lipid droplet-binding adipocyte differentiation-related protein. J Biol Chem 2003;278:15998–16007. https://doi.org/10.1074/jbc.M211289200.
[27] Schratter M, Lass A, Radner FPW. ABHD5-A regulator of lipid metabolism essential for diverse cellular functions. Metabolites 2022;12:1015. https://doi.org/10.3390/metabo12111015.
[28] Krahmer N, Guo Y, Wilfling F, et al. Phosphatidylcholine synthesis for lipid droplet expansion is mediated by localized activation of CTP:phosphocholine cytidylyltransferase. Cel Metab 2011;14:504–515. https://doi.org/10.1016/j.cmet.2011.07.013.
[29] Menzel N, Fischl W, Hueging K, et al. MAP-kinase regulated cytosolic phospholipase A2 activity is essential for production of infectious hepatitis C virus particles. PLoS Pathog 2012;8:e1002829. https://doi.org/10.1371/journal.ppat.1002829.
[30] Rubbia-Brandt L, Quadri R, Abid K, et al. Hepatocyte steatosis is a cytopathic effect of hepatitis C virus genotype 3. J Hepatol 2000;33:106–115. https://doi.org/10.1016/s0168-8278(00)80166-x.
[31] Vogt DA, Camus G, Herker E, et al. Lipid droplet-binding protein TIP47 regulates hepatitis C Virus RNA replication through interaction with the viral NS5A protein. PLoS Pathog 2013;9:e1003302. https://doi.org/10.1371/journal.ppat.1003302.
[32] Abenavoli L, Masarone M, Peta V, et al. Insulin resistance and liver steatosis in chronic hepatitis C infection genotype 3. World J Gastroenterol 2014;20:15233–15240. https://doi.org/10.3748/wjg.v20.i41.15233.
[33] Khan M, Jahan S, Khaliq S, et al. Interaction of the hepatitis C virus (HCV) core with cellular genes in the development of HCV-induced steatosis. Arch Virol 2010;155:1735–1753. https://doi.org/10.1007/s00705-010-0797-7.
[34] **Sztalryd C**, **Xu G**, Dorward H, et al. Perilipin A is essential for the translocation of hormone-sensitive lipase during lipolytic activation. J Cel Biol 2003;161:1093–1103. https://doi.org/10.1083/jcb.200210169.
[35] **Youssefian L**, **Vahidnezhad H**, Saeidian AH, et al. Inherited non-alcoholic fatty liver disease and dyslipidemia due to monoallelic ABHD5 mutations. J Hepatol 2019;71:366–370. https://doi.org/10.1016/j.jhep.2019.03.026.
[36] Lin W, Tsai WL, Shao RX, et al. Hepatitis C virus regulates transforming growth factor beta1 production through the generation of reactive oxygen species in a nuclear factor kappaB-dependent manner. Gastroenterology 2010;138:2509–2518.e1. https://doi.org/10.1053/j.gastro.2010.03.008.
[37] Yoshida H, Kato N, Shiratori Y, et al. Hepatitis C virus core protein activates nuclear factor kappa B-dependent signaling through tumor necrosis factor receptor-associated factor. J Biol Chem 2001;276:16399–16405. https://doi.org/10.1074/jbc.M006671200.
[38] Sato Y, Kato J, Takimoto R, et al. Hepatitis C virus core protein promotes proliferation of human hepatoma cells through enhancement of transforming growth factor alpha expression via activation of nuclear factor-kappaB. Gut 2006;55:1801–1808. https://doi.org/10.1136/gut.2005.070417.
[39] Li S, Ye L, Yu X, et al. Hepatitis C virus NS4B induces unfolded protein response and endoplasmic reticulum overload response-dependent NF-kappaB activation. Virology 2009;391:257–264. https://doi.org/10.1016/j.virol.2009.06.039.
[40] **Gong G**, **Waris G**, Tanveer R, et al. Human hepatitis C virus NS5A protein alters intracellular calcium levels, induces oxidative stress, and activates STAT-3 and NF-kappa B. Proc Natl Acad Sci USA 2001;98:9599–9604. https://doi.org/10.1073/pnas.171311298.
[41] Liao QJ, Ye LB, Timani KA, et al. Hepatitis C virus non-structural 5A protein can enhance full-length core protein-induced nuclear factor-kappaB activation. World J Gastroenterol 2005;11:6433–6439. https://doi.org/10.3748/wjg.v11.i41.6433.
[42] Kitamura M. Control of NF-κB and inflammation by the unfolded protein response. Int Rev Immunol 2011;30:4–15. https://doi.org/10.3109/08830185.2010.522281.

Keywords: HCV; liver steatosis; human hepatocyte chimeric mice; lipidome analysis; PLA2G4C.
*Received 31 May 2024; received in revised form 17 September 2024; accepted 25 September 2024; Available online 30 September 2024*